Simulation of cavitating flow in high pressure gasoline injectors

D. Greif[1], B. Monteverde[2], A. Alajbegovic[3]

1. AVL AST d.o.o., Partizanska 13a, 2000 Maribor, Slovenia
2. Magneti Marelli, Bologna, Italy
3. AVL Powertrain Engineering Inc., 47519 Halyard Drive, Plymouth, MI 48170-2438, USA

Presented is a multidimensional model for predicting cavitating flow in a “multi-hole” high pressure fuel injector. This technology is of potential interest to high performance environment such as in Formula 1 direct-injection spark ignited engines. The applied computational model is based on the two-fluid model and has been implemented into *AVL-FIRE*, a Computational Fluid Dynamics (CFD) code. The model simulates *n*-phase flow systems. The components considered in the presented work were liquid gasoline and gasoline vapor. Cavitation in injection systems is desired to a certain degree because the collapse of cavitation bubbles influences the turbulence intensity towards the outlet of the injection holes. This consequently enhances the break-up process in the combustion chamber. At the same time, correct prediction of the cavitation phenomena is very important in order to avoid cavitation erosion, to estimate the discharge rates under cavitating conditions, and to estimate the force on the needle (to design the regulation mechanism of the injection system). The presented methodology can be used to simulate flows in different types of gasoline and diesel injectors. Single- and multi-phase simulations using different meshing techniques have been performed; the first approach featuring a "hand-made" structured computational grid with arbitrary interface connections, and the second one using an automatically generated unstructured hybrid grid. Predicted discharge rates were found to be in good agreement with the measurements.

Keywords: cavitation, injector, gasoline.

1. Introduction

Fuel injection is essential for the operation and performance of internal combustion (IC) engines. High pressure fuel injectors are used in both Diesel and Direct Gasoline Injection (DGI) engines. The present work considers the gasoline injector type.

Direct injection Otto engines exhibit a high potential for reduction of fuel consumption. Throughout the entire range of operation a combustible mixture must be present at the spark plug. Computational Fluid Dynamics (CFD) simulations combined with experiments prove to be a good tool to test many configurations in a short time, to test different injectors, as well as to vary the operational parameters, such as injector positions, injection timing, duration, etc.
Nowadays fuel injection for Diesel applications is performed at very high inlet pressures that range from 200 to 2000 bar. During recent years passenger car manufacturers have been

testing Direct Injection (DI) gasoline injectors with injection pressures ranging from 100 – 300 bar. The purpose of such high inlet pressures is to produce high injection velocities that a.) result in an efficient atomization process with small droplets and b.) traverse rapidly through the combustion chamber (Haywood [1]). Due to high velocities in injection nozzles it is quite common to observe cavitation. This has a desirable effect by further enhancing the atomization process. At the same time, uncontrolled cavitation can result in considerable surface erosion due to bubble collapse close to injector walls, thus reducing the lifetime of the injection system.

Presented is a flow study of a high pressure gasoline injector designed to operate in direct-injection spark engines. Currently Formula 1 racing teams are particularly interested in this technology. The bottom part of the injector looks somewhat like a sac hole type of a Diesel injector. The upper part of the injector differs completely from the diesel injector design. It is important to note that gasoline enters a separate inlet chamber through which it is delivered to the needle chamber.

Here a multiphase flow model is considered that can be used for the simulation of both Diesel and DGI injectors. The computational tool used was the commercial CFD code AVL FIRE. The injector was simulated both as single- and two-phase flow system. In the two-phase system both liquid and vapor created by cavitation were taken into account. Flow is simulated up to the exit of the injection nozzle. The model applied in the present study can be extended to an *n*-phase system (Alajbegovic et al. [2]) and is capable of simulating a wide range of nozzle flows encountered in internal combustion engines.

Two types of computational grids were applied featuring structured domain parts connected by arbitrary interfaces in the first case and an unstructured grid generated through a fully automated process in the second case.

2. Theoretical background

The model is based on the multi-fluid formulation for multi-phase flows (Drew & Passman [6]; Lahey & Drew [7]). Numerical approach to the simulation of multi-phase flow was provided by Kunz et al. [8] and Carrica et al. [9]. The implemented model can be applied for *n*-phase flows, and here it is reduced to a two-phase case since only two phases are present.
Mass conservation equation is equal to:

$$\frac{\partial a_k r_k}{\partial t} + \nabla \cdot a_k r_k \mathbf{v}_k = \sum_{l=1, l\neq k}^{2} \Gamma_{kl} \qquad (1)$$

The phases are numbered as fuel liquid (1), and fuel vapor (2). Both components are assumed incompressible. The compressibility has only a minor effect on the volume fraction generation. This has been verified by comparing the predictions with the experimental data (Alajbegovic et al. [5]). In the present case cavitation occurs within the fuel component. Mass exchange is approximated using the simplified Rayleigh equation (Grogger & Alajbegovic [10]):

$$\Gamma_{12} = r_1 N''' 4\pi R^2 \frac{\partial R}{\partial t} = -\Gamma_{21} \qquad (2)$$

N''' is the bubble number density and is calculated according to the following formula:

$$N''' = \begin{cases} N_0''' & a_2 \le 0.5 \\ 2(N_0''' - 1)(1 - a_2) + 1 & a_2 > 0.5 \end{cases} \tag{3}$$

This is a rather heuristic formula used to model coalescence effects at higher volume fraction levels. The initial number density, N_{init}''', was 10^{12} as suggested by Fujimoto et al. [11]. In addition, the compatibility condition has to be fulfilled:

$$\sum_{k=1}^{2} a_k = 1 \tag{4}$$

Momentum conservation equation equals:

$$\frac{\partial a_k \rho_k \mathbf{v}_k}{\partial t} + \nabla \cdot a_k \rho_k \mathbf{v}_k \mathbf{v}_k = -a_k \nabla p + \nabla \cdot a_k (\tau_k + \tau_k^t) + a_k \rho_k \mathbf{g} + \sum_{l=1, l \neq k}^{2} \mathbf{M}_{kl} + \sum_{l=1, l \neq k}^{2} \mathbf{v}_k \Gamma_{kl} \tag{5}$$

where τ_k is viscous shear stress and τ^t_k is Reynolds stress. The interfacial momentum transfer between phases k and l, M_{kl}, includes drag and turbulent dispersion forces:

$$\mathbf{M}_{kl} = C_{TD} \rho_k k_k \nabla a_l + C_D \frac{1}{8} \rho_k A_i''' |\mathbf{v}_r| \mathbf{v}_r = -\mathbf{M}_{lk} \tag{6}$$

Assumed is uniform pressure field for all phases:

$$p_k = p, \quad k = 1,2 \tag{7}$$

Turbulence conservation equation is solved for each phase:

$$\frac{\partial a_k \rho_k k_k}{\partial t} + \frac{\partial a_k \rho_k k_k v_{k,l}}{\partial x_l} = a_k \rho_k P_k + \frac{\partial}{\partial x_l}\left(a_k \rho_k \frac{C_m}{\sigma_k} \frac{k_k^2}{\varepsilon_k} \frac{\partial k_k}{\partial x_l} \right) - a_k \rho_k \varepsilon_k + \sum_{l=1, l \neq k}^{2} k_k \Gamma_{kl} \tag{8}$$

where P_k is the production term. Turbulence dissipation equation equals:

$$\begin{aligned} \frac{\partial a_k \rho_k \varepsilon_k}{\partial t} + \frac{\partial a_k \rho_k \varepsilon_k v_{k,j}}{\partial x_j} = & -\rho_k a_k C_{\varepsilon 1} \frac{\overline{v'_{k,i} v'_{k,j}}}{k_k} \frac{\partial v_{k,i}}{\partial x_j} \varepsilon_k - \rho_k a_k C_{\varepsilon 2} \frac{\varepsilon_k^2}{k_k} \\ & + \frac{\partial}{\partial x_j}\left(\rho_k a_k \frac{C_\varepsilon k_k}{\varepsilon_k} \overline{v'_{k,j} v'_{k,l}} \frac{\partial \varepsilon_k}{\partial x_l} \right) + \sum_{l=1, l \neq k}^{2} \varepsilon_k \Gamma_{kl} \end{aligned} \tag{9}$$

Standard values for the closure coefficients in turbulence kinetic energy and turbulence dissipation equations are used. The model has been implemented into the AVL FIRE commercial CFD code. The values for closure coefficients can be found in [13].

3. Different meshing techniques

Two types of computational grids were used. In the first case, structured parts of the domain were connected with arbitrary interface technology. Figure 1 shows the computational grid

with three arbitrary interface connections. Total number of internal cells was 102,760. Overall meshing effort was 5 hours.

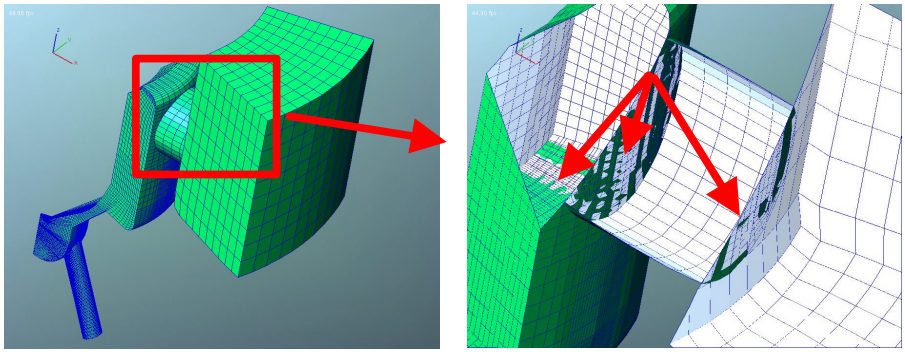

Figure 1. Structured parts connected with arbitrary interfaces.

Recently automated meshing technology using AVL FAME offers a great reduction in the effort required for grid generation. The grid is entirely unstructured and it consists of 118,941 internal cells, meshing effort was reduced to half an hour. Figure 2 shows the automatically generated computational mesh.

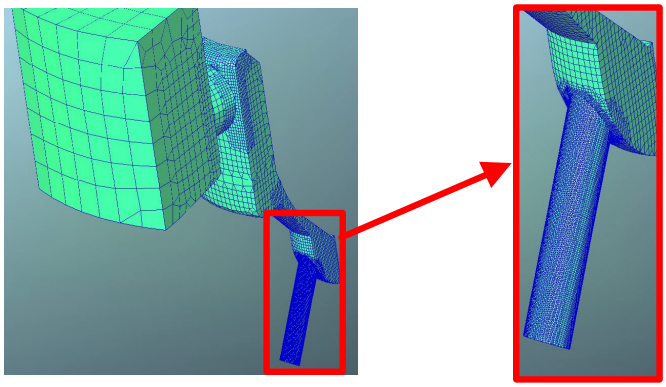

Figure 2. Fully automated meshing approach using AVL CFDWM.

4. Boundary conditions and the material data

Figure 3 shows the boundary conditions used in the simulations. Due to symmetry only one segment was calculated to reduce computational complexity. Pressure at the inlet was set to 501 bar, while the outlet pressure was set to the atmospheric value at 1bar. Symmetry boundary conditions were applied on both sides of the model.

Table 1 shows the important gasoline properties for a liquid phase and for its vapor phase as well.

Table 1. Gasoline data.

	Liquid phase	Vapor phase
Density [kg/m^3]	727.4	0.113
Dynamic viscosity [kg/m*sec]	4.8e-4	6.3e-6
Vapor pressure [Pa]	2512	

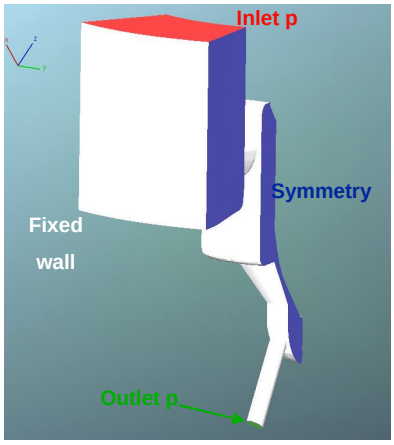

Figure 3. Boundary conditions.

5. Simulation results

Presented simulation results are focused on the area around the injection hole. This is physically the most important and interesting area. Simulations were performed as transient until steady state conditions were reached and the results presented here feature such flow conditions. Magneti Marelli, the injector manufacturer, reported experimentally measured steady flow rate of 38 - 40 g/s.

5.1. Single-phase results

The results of the single-phase simulations showed very low pressure levels in the area of the injection hole inlet. Calculated flow rate was over-predicted at 49.6 g/sec. Both observations indicate that cavitation will take place and result in choked flow conditions. Figure 4 shows the velocity for the liquid phase (a) and the turbulence kinetic energy (TKE) (b) in the injection hole area. The three cuts show the distributions on an axial cut, on radial cuts along the injection hole axis, and on the injector surface. Maximum velocity magnitude reaches 382 m/s, while maximum TKE reaches 344 m^2/s^2.

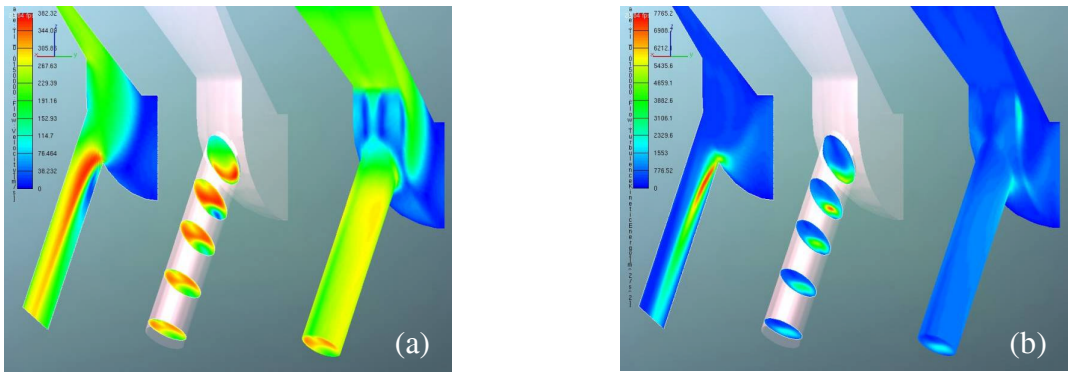

Figure 4. Velocity (a) and turbulence kinetic energy (b).

5.2. Multi-phase results on a structured grid with arbitrary interface connections

Two phases were accounted for; gasoline liquid and gasoline vapor. Vapor generation is driven by the local pressure falling below the vapor pressure of gasoline at the given temperature. The threshold for the cavitation mass-transfer was 2512 Pa. As expected from the single phase simulation, the local pressure caused by liquid acceleration around the entrance into the injection hole decreased below the vapor pressure and cavitation took place. Calculated flow rate was 38 g/s which is in agreement with the measurements.

Figure 5 (a) shows the phase distribution on the same cross-sections as for the presentation of the single-phase flow results. Volume fraction indicates the locations of vapor (red color). The cross-sectional area is partially blocked by the vapor-cloud, which is split into two "sleeves" due to the secondary liquid motion. The phenomena is shown in Figure 5 (b). The picture on the left shows the iso-surface of 50%, while the picture on the right shows the phase distribution from a slightly different view angle onto the injection hole. The vapor region extends into the outlet plane. Cavitation at the outlet plane of the injection hole influences the spray distribution in the combustion chamber and enhances the break-up process as detected by Von Berg et. al. [12].

Figures 6 (a) and (b) show the velocity and the turbulence kinetic energy for the liquid phase respectively. Maximum liquid velocity compared with the single-phase simulation is 344 m/s. This value is lower although the cross-sectional area is partially blocked by the vapor zone. This happens due to the choked flow conditions caused by the onset of cavitation.

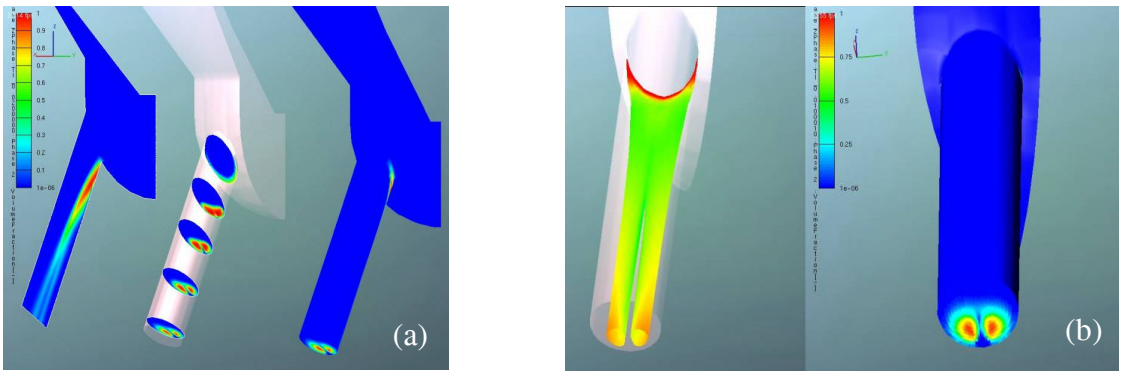

Figure 5. Volumetric fraction in the injection hole area (blue – liquid, red – vapor) (a), split cavitation (b).

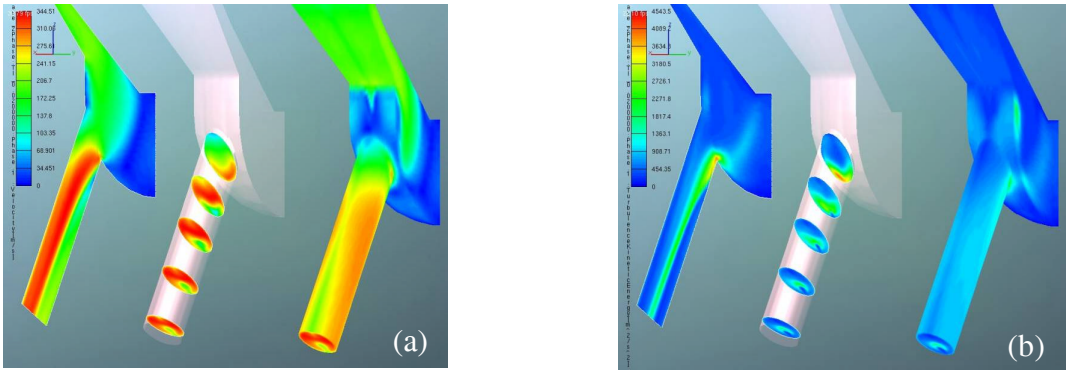

Figure 6. Velocity (a) and turbulence kinetic energy (b) for the liquid phase.

5.3. Multi-phase results on an unstructured grid

In general, the results on the unstructured grid show the same discharge rate, same velocity and turbulence levels, and the same volume fraction.

Figure 7 shows the phase distribution on the characteristic cuts. Split cavitation was again detected. Figure 8 shows the velocity and the turbulence level in the injection hole.

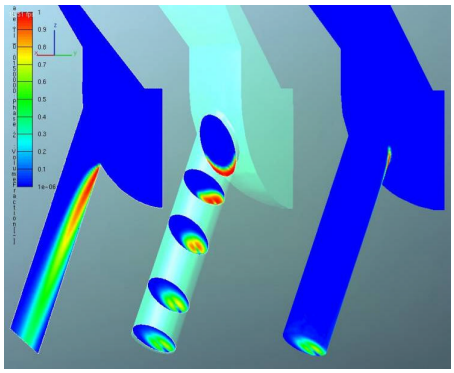

Figure7. Volumetric fraction in the injection hole area (blue – liquid, red – vapor).

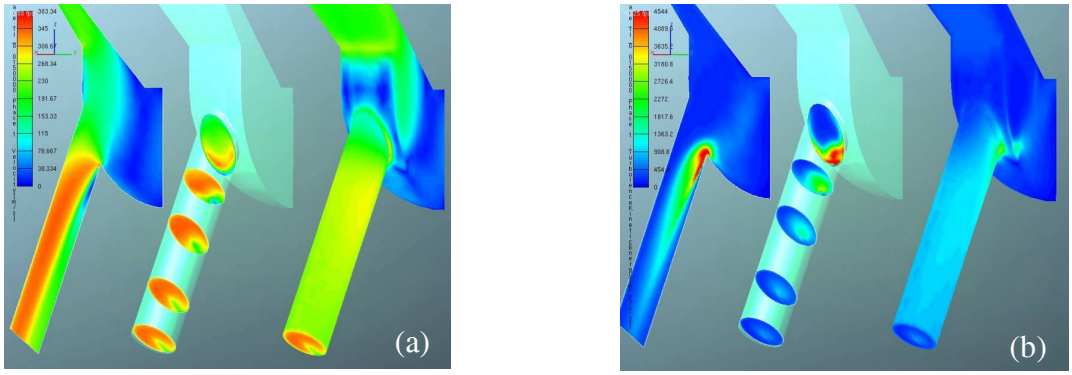

Figure 8. Velocity (a) and turbulence kinetic energy (b) for the liquid phase.

5. Conclusions

Presented was a multiphase flow model for the simulation of high-pressure gasoline injector. This technology is a big challenge for the future and is currently of interest for Formula 1 teams. Calculated three-dimensional results of the flow in an injector were shown using different meshing techniques. Single-phase results demonstrated an over-predicted flow-rate, meaning that choked flow conditions (resulting from cavitation) were not accounted for in the single phase simulation. This assumption proved to be correct since the two-phase cavitating flow simulation resulted in an agreement with the experiment.

Fully automated meshing approach using AVL FAME lead to an extreme reduction of grid-generation effort. The results demonstrated that the implemented numerical model can be used to simulate flows in injectors under conditions that can be observed in state-of-the-art internal combustion engines. Mass-transfer due to cavitation was detected, therefore the multi-phase type of simulation is essential in order to obtain realistic results.

6. References

[1] Haywood, J.B., Internal Combustion Engine Fundamentals, McGraw-Hill, New York, 1988.

[2] Alajbegvic A., Meister G., Greif D., Basara B., Three phase cavitating flows in high pressure swirl injectors, *ETF Science 26 (2002),* 677-681.

[3] Kunz, R.F., Boger, D.A., Stinebring, D.R., Chyczewski, T.S., Gibeling, H.J., Govindan, T.R., Multi-phase CFD Analysis of Natural and Ventilated Cavitation About Submerged Bodies, *FEDSM99*-7364 (1999).

[4] Kunz, R.F., Boger, D.A., Stinebring, D.R., Chyczewski, T.S., Gibeling, H.J., Venkateswaran, S., Govindan, T.R., A Preconditioned Navier-Stokes method for Two-Phase Flows with Application to Cavitation prediction, *Computers and Fluids* **29** (8) (2000) 849-875.

[5] Alajbegovic, A., Grogger, H.A., Philipp, H., "Calculation of Transient Cavitation in Nozzle Using the Two-Fluid Model," *ILASS-99 Conference Proceedings* (1999).

[6] Drew, D.A., Passman, S.L., Theory of Multicomponent Fluids, *Springer, New York*, 1998.

[7] Lahey, R.T., Jr., Drew, D.A., An Analysis of Two-Phase Flow and Heat Transfer Using a Multidimensional, Multi-Field, Two-Fluid Computational Fluid Dynamics (CFD) Model, *Japan/US Seminar on Two-Phase Flow Dynamics*, Santa Barbara, California (2000).

[8] Kunz, R.F., Siebert, B.W., Cope, W.K., Foster, N.F., Antal, S.P., Ettore, S.M., A Coupled Phasic Exchange Algorithm for Multi-Dimensional Four-Field Analysis of Heated Flows with Mass Transfer, *Computers and Fluids* **27** (7) (1998) 741-768.

[9] Carrica, P.M., Bonetto, F., Drew, D.A., Lahey, R.T., Jr., A Polydispersed Model for Bubbly Two-Phase Flow Around a Surface Ship, *Int. J. Multiphase Flow* **25** (2) (1999) 257-305.

[10] Grogger, H., Alajbegovic, A., Calculation of the Cavitating Flow in Venturi Geometries using Two Fluid Model, *FEDSM98*-5295 (1998).

[11] Fujimoto, H., Mishikori, T., Tsumakoto, T., and J. Senda, Modeling of Atomization and Vaporization Process in Flash Boiling Spray, *ICLASS*-94, paper VI-13 (1994).

[12] E. v. Berg, D. Greif, R. Tatschl, E. Winklhofer, L. C. Ganippa, Primary break-up model for diesel jets based on locally resolved flow field in the injection hole, *ILASS – Europe 2002*, Zaragoza (2002)

[13] AVL FIRE Multiphase Flow Manual, AVL List GmbH, January 2003